NIGHTTIME ATMOSPHERIC STABILITY CHANGES AND THEIR EFFECTS ON THE TEMPORAL INTENSITY OF A MESOSCALE CONVECTIVE COMPLEX

Jeffrey S. Hovis

and

Kenneth C. Brundidge

Texas A&M University

College Station, Texas

Prepared for George C. Marshall Space Flight Center

under Grant NAG8-043

ABSTRACT

Nighttime Atmospheric Stability Changes and their Effects on the Temporal Intensity of a Mesoscale Convective Complex.

A method of interpolating atmospheric soundings while reducing the errors associated with simple time interpolation was developed. The purpose of this was to provide a means to determine atmospheric stability at times between standard soundings and to relate changes in stability to intensity changes in an MCC. Four MCC cases were chosen for study with this method with four stability indices being included.

At this time, the study of all four cases is incomplete and only the preliminary results for Case 1 are described. The discussion centers on three aspects for each stability parameter examined: the stability field in the vicinity of the storm and its changes in structure and magnitude during the lifetime of the storm, the average stability within the storm boundary as a function of time and its relation to storm intensity, and the apparant flux of stability parameter into the storm as a consequence of low-level storm relative flow. It was found that the results differed among the four stability parameters, sometimes in a conflicting fashion. Thus, an interpolation of how the storm intensity is related to the changing environmental stability depends upon the particular index utilized. Some explanation for this problem is offered.

ACKNOWLEDGEMENTS

The work reported upon here was in part supported by the National Aeronautics and Space Administration under the auspices of the Atmospheric Sciences Division, Space Sciences Laboratory, Marshall Space Flight Center under Grant NAG8-043.

TABLE OF CONTENTS

LIST OF TABLES

LIST OF FIGURES

I. INTRODUCTION

Mesoscale Convective Complexes (MCCs) have recently been receiving considerable attention from the meteorological research community. The research on MCCs seems to have blossomed since these long-lived thunderstorm systems were defined by Maddox (1980) on the basis of their appearance in satellite imagery coupled with cloud top temperatures of their convective elements.

MCCs are important features in the weather of the midwestern section of the United States. Fritsch et al. (1981) found that these storms were responsible for a large percentage of the rainfall in this area. Several researchers (Maddox et al., 1982; Rodgers et al., 1983) have found that they also produce a significant amount of severe weather including flash floods, tornadoes, high winds, and hail, which cause many deaths, injuries, and significant property damage.

Four groups of researchers (Maddox, 1981; Maddox et al., 1982; Rodgers et al., 1983; Rodgers et al., 1985) have studied the life cycle of these storms by using the criteria set up by Maddox (1980). The first storms were found to form, on average, in the midafternoon about 2100 GMT. The storm was found to build in size with time and usually to meet the definition of an MCC at approximately 0300 GMT, which corresponds to the nighttime hours in the midwest. The maximum extent and intensity were reached in the early morning hours at about 0800 GMT. The time of 1230 GMT was the approximate time of termination, in the sense that the storm no longer met the definition of an MCC. Thus, while the average life span of an MCC as such

was about 9 h, convective storm activity associated with the system could last much longer.

Several researchers have shown that upper air observations at 12-h intervals are inadequate for the study of short-lived mesoscale processes. House (1960) concluded that the upper air network with an average spacing between observations of 220 n mi and time spacing of 12 h was insufficient to resolve the mesoscale features that led to the formation, movement, and dissipation of squall lines. Kreitzburg and Brown (1970) showed the mesoscale features within the synoptic scale flow could be linked to the variability of the weather. When looking at a continental occlusion with rawinsonde observations at 90-min intervals they found synoptic-scale features, while having continuity of days in time and around 1000 mi in space, contained mesoscale features with time continuity of a few hours and space continuity of a few hundred miles.

Wilson and Scoggins (1976) studied the atmosphere using rawinsonde observations taken during AVE (Atmospheric Variability Experiment) II. They found that between 30-60% of the total change in atmospheric variables observed over the 12-h period occur within a 3-h interval. In several cases the 3-h changes were larger than those measured over 12 h. As a matter of fact, large changes of vertical motion and potential instability can lead to a change in convective activity by a factor of more than seven over that found in the 12-h data.

Dupuis and Scoggins (1979) used a linear time interpolation scheme to estimate the structure of the atmosphere over the regular 12-h interval between rawinsonde observations. These interpolated values were compared with the actual 3-h observations. They found that the magnitudes of the non-linear changes were largest in areas of convection. The instability increased non-linearly in areas of convection as did low-level convergence and upward vertical motion. This was determined to be important in the release of the potential instability. They concluded that linear time interpolation was inadequate in defining variability over time of atmospheric parameters.

Since vorticity and atmospheric stability are important parameters in convection, Read and Scoggins (1977) used 3-h rawinsonde data from AVE IV to compare the 3-h changes of these parameters to those measured over 12 h for the same time period. Instability was found to be greatest at 3 h prior to thunderstorm development. This would hardly be seen with conventional 12-h observations. Changes in the magnitudes of terms in the vorticity equation also were found to be larger in the 3-h data than that found in the 12-h data. They concluded that the changes in the vorticity, stability, and intensity of the convection over the 3-h periods indicated that studies of convective activity could not be adequately done using 12-h observations.

Vertical motion variability between 3-h and 12-h rawinsonde data has been studied by Overall and Scoggins (1975). Vertical motion had been determined to be important in enhancing and maintaining convective activity by Byers (1944). So, unseen changes in vertical motion could lead to unexplained occurrences of convection. Overall and Scoggins found that

changes in vertical motion for 3-h data could be as large as four times that found when looking at 12-h observations. They also found that the number of mesoscale features that could be analyzed increased as the interval between rawinsonde observations decreased from 12 to 3 h.

Since the MCC is predominantly a nocturnal event, daytime heating does not play an important role in the maintaining of the MCC intensity. So, some other important feature, such as atmospheric stability aloft, must play a significant role in controlling the intensity of the MCC during the nighttime. Considering all this information, research was performed with the following objectives in mind.

(1) to develop a method of interpolating atmospheric soundings to 500 mb between the standard observation times, and

(2) to use these interpolated soundings to examine how the changing stability of the atmosphere in the environment of a Mesoscale Convective Complex (MCC) is related to its temporal intensity changes.

II. PROCEDURE

In order to obtain reasonably accurate interpolated atmospheric soundings, the following was done.

Two AVE-SESAME (Atmospheric Variability Experiment- Severe Environmental Storms and Mesoscale Experiment) data sets were obtained in which radiosonde observations were taken at 3-h intervals for 00 through 12 GMT.

Initially, the data sets were analyzed to separate them into three different groups (storm, non-storm, and all stations). This separation was done by utilizing radar summary maps for the periods involved. If a station had rain or a thunderstorm located within approximately 50 km of it during the period of 2235 GMT from the previous day to 1235 GMT of the day of interest, the station was classified as a storm case. Otherwise, it was a non-storm case. Once this was done, the following interpolation routines were applied to each of these new data sets.

Linear interpolation in time at 25 mb intervals up to 500 mb, not including the surface level, was then performed between the 00 and the following 12 GMT observations to obtain values of temperature and mixing ratio at 03, 06, and 09 GMT. These interpolated values were compared to the actual measured values in order to identify a level of least average error for each of the times.

Vertical interpolation in pressure was then performed using the values at the levels of least average error and the observed values at the surface. This process was carried out from the surface to the 500 mb level at 25 mb intervals also.

In order to incorporate both interpolation methods into one general method, the values obtained from the two interpolations (time and pressure) at each reported time and every level were then matched with the actual measured values to get a least squares fit to the observed data. Three sets of coefficients (storm, non-storm, and all stations) were obtained for use in the resulting interpolation equations. An estimate of the accuracy of the resulting interpolation relationships for temperature and mixing ratio was then obtained by applying them to another AVE-SESAME data set. Also, the results were then examined to see if there is any significant benefit in having separate interpolation equations for storm and non-storm location.

After the interpolation relationships had been determined, they were applied to data sets from areas around MCCs that had previously been identified by Welshinger (1985). Each data set included all upper air stations with available data that were within several hundred kilometers of the location of the MCC.

In order for a station to be used, upper air data, including mandatory and significant levels up to 500 mb, had to be available. Also, the station had of have surface data for 03, 06, and 09 GMT for the time period of interest, including temperature, dewpoint temperature, and sea level pressure or altimeter setting.

Various stability indices were then calculated and plotted on maps showing the air flow in and around the MCC. These indices, including the K index, Total-Totals, CAPE (Convective Available Potential Energy), and the maximum rate of decrease of equivalent potential temperature over a 25 mb layer from the surface to 700 mb (PII- Potential Instability Index), showed the stability of the environmental air feeding the storm and how it changed through the lifetime of the MCC.

The intensity of the MCC as a function of time was indicated by the area enclosed by given values of cloud-top temperatures obtained through satellite measurements. This was in keeping with the criteria established by Maddox (1980).

III. RESULTS

Interpolation Procedure

In an attempt to reduce the errors associated with linear time interpolation, interpolation with respect to pressure was also utilized. This procedure would allow changes at the surface to influence the final soundings. Table 1 shows an example of the errors associated with time interpolation and interpolation with respect to pressure. In the lowest layers, the errors associated with each method are similar. But above that level, time interpolation is much better.

In order to combine the two procedures and reduce the errors to a minimum, a least-squares fit was applied to the interpolated values at various pressure levels and various times. An example of the coefficients for the interpolation equations that resulted after the least-squares fit was applied is given in Table 2. An example of the actual interpolation equation is

$$Q = a_0 + a_1 Q_t + a_2 Q_p$$

where Q_t and Q_p represent the values of the given quantity obtained from time interpolation and pressure interpolation, respectively. Once these coefficients were determined, the interpolation relationships were tested on the original data set to see how much improvement over linear time interpolation was found. Table 3 gives a comparison of the errors resulting from simple time interpolation in comparison to the errors resulting from the new method. For this purpose, the absolute values of the errors on

Table 1. Absolute error analysis of the original data set for the two interpolation methods for temperature at 0600 GMT. All values are in C°.

Pres (mb)	Time interpolation		Pressure interpolation	
	Mean errors	Standard deviations	Mean errors	Standard deviations
1000	0.8	0.56	0.4	0.34
975	1.0	0.65	1.2	1.09
950	1.3	1.05	1.3	1.54
925	1.5	1.24	1.5	1.72
900	1.6	1.65	2.1	2.23
875	1.6	1.86	2.5	2.57
850	1.6	1.68	3.1	2.81
825	1.6	1.52	3.4	2.94
800	1.8	1.56	4.0	3.05
775	1.9	1.68	5.0	2.92
750	1.7	1.30	6.0	2.86
725	1.6	1.08	6.1	2.70
700	1.2	0.93	5.8	2.51
675	1.1	0.91	5.4	2.35
650	0.9	0.74	5.0	1.93
625	0.9	0.74	4.3	1.64
600	1.0	0.97	3.4	1.53
575	1.1	1.01	2.5	1.24
550	1.0	0.80	1.6	0.98
525	1.0	0.89	1.0	0.89
500	1.1	0.91	1.4	1.23

TABLE 2. Least squares coefficients for temperature and mixing ratio to be used to interpolate the 0600 GMT soundings.

	Temperature			Mixing ratio		
Pres (mb)	a_0	a_1	a_2	a_0	a_1	a_2
1000	14.34	0.84	−0.51	2.10	0.72	0.18
975	−0.41	0.71	0.31	−0.52	0.49	0.58
950	0.43	0.56	0.43	0.48	0.18	0.82
925	0.47	0.46	0.55	0.21	0.24	0.80
900	0.92	0.55	0.43	−0.42	0.64	0.44
875	1.51	0.55	0.39	0.00	0.76	0.28
850	0.86	0.73	0.23	1.05	0.94	−0.04
825	0.11	0.85	0.15	0.71	0.72	0.22
800	0.54	0.81	0.20	1.52	0.69	0.11
775	0.13	0.88	0.24	2.49	0.78	−0.28
750	0.17	0.95	0.21	3.32	0.74	−0 48
725	0.48	0.96	0.19	4.21	0.54	−0.63
700	0.56	0.96	0.17	3.70	0.52	−0.60
675	0.53	1.00	0.07	3.23	0.60	−0.67
650	0.83	0.94	0.11	2.23	0.80	−0.61
625	1.15	0.85	0.19	1.12	0.88	−0.42
600	1.11	0.80	0.24	0.96	0.79	−0.43
575	1.68	0.50	0.55	0.30	0.61	−0.08
550	0.74	0.66	0.35	0.20	−1.75	2.22
525	0.35	1.97	−0.96	0.24	0.42	0.20
500	0.15	0.96	0.05	0.13	0.69	0.05

Table 3. Absolute error analysis of the original data set of the two interpolation methods for temperature at 0600 GMT. All values are in C°.

Pres (mb)	Time interpolation		New method	
	Mean errors	Standard deviations	Mean errors	Standard deviations
1000	0.8	0.56	0.1	0.11
975	1.0	0.65	0.8	0.56
950	1.3	1.05	1.1	0.98
925	1.5	1.24	1.3	1.07
900	1.6	1.65	1.6	1.33
875	1.6	1.86	1.6	1.43
850	1.6	1.68	1.6	1.54
825	1.6	1.52	1.5	1.22
800	1.8	1.56	1.7	1.36
775	1.9	1.68	1.8	1.35
750	1.7	1.30	1.5	1.07
725	1.6	1.08	1.3	1.04
700	1.2	0.93	1.0	0.90
675	1.1	0.91	1.0	0.87
650	0.9	0.74	0.8	0.65
625	0.9	0.74	0.7	0.67
600	1.0	0.97	0.9	0.88
575	1.1	1.01	1.0	0.87
550	1.0	0.80	0.9	0.81
525	1.0	0.89	1.0	0.87
500	1.1	0.91	1.0	0.92

each pressure surface were averaged. The reduction in error associated with the new method is significant. If one considers an algebraic average on each pressure surface, the resulting errors are approximately zero (not shown here). This is what we would expect after applying a least-squares fit to the data. However, this does not quarantee the efficacy of the procedure when applied to independent data. Therefore, as a test of the procedure, it was applied to a third AVE-SESAME case. For the new method to be considered good, the errors associated with this new case should be small. Also, the standard deviations should be small. In Tables 4-6, the errors in temperature associated with simple interpolation in time and the new technique are compared. For this purpose, there has been no separation into storm vs non-storm soundings.

At 03 GMT (Table 4), it can be seen that between 1000 and approximately 900 mb, the new method appears to be better than linear time interpolation. Above that level, the two methods have similar errors, with neither providing a distinct advantage. Similar results are seen in Tables 5 and 6.

The results for the mixing ratio (Table 7-9) are quite similar to those for the temperature calculation. Again, the new method shows some advantage in the boundary layer where the influence of values at the surface is the greatest. However, above the boundary level, simple interpolation in time gives somewhat smaller errors.

The conclusion reached from these comparisons was that the smaller errors provided by the interpolation relationships (Table 2) in the boundary layer was of greater significance for the purpose of this study than the slight advantage gained by using linear time interpolation in the upper

Table 4. Absolute error analysis of the two interpolation methods for temperature at 0300 GMT. All values are in C°.

Pres (mb)	Time interpolation		New method	
	Mean errors	Standard deviations	Mean errors	Standard deviations
1000	1.2	0.86	0.5	0.28
975	0.8	0.47	0.7	0.56
950	1.7	2.67	1.5	2.05
925	2.0	2.48	1.7	1.75
900	1.6	1.59	1.5	1.47
875	1.3	0.92	1.2	1.09
850	1.2	0.97	1.3	1.07
825	1.3	0.81	1.3	0.96
800	1.0	0.65	1.0	0.73
775	0.9	0.62	1.2	0.81
750	0.9	0.59	0.9	0.60
725	0.8	0.58	0.8	0.53
700	0.8	0.59	0.8	0.60
675	0.8	0.78	0.9	0.79
650	0.8	0.76	0.8	0.78
625	0.7	0.60	0.8	0.70
600	0.8	0.68	0.8	0.70
575	0.9	0.77	1.0	0.80
550	1.1	1.00	1.2	1.01
525	1.0	0.92	1.0	0.86
500	1.0	0.92	0.9	0.88

Table 5. Absolute error analysis of the two interpolation methods for temperature at 0600 GMT. All values are in C°.

Pres (mb)	Time interpolation		New method	
	Mean errors	Standard deviations	Mean errors	Standard deviations
1000	1.1	0.63	0.9	0.49
975	2.0	1.81	1.6	1.19
950	2.3	2.19	1.9	1.38
925	2.4	2.21	2.2	1.51
900	1.8	1.81	1.8	1.44
875	1.7	1.42	1.7	1.47
850	1.2	1.13	1.3	1.30
825	1.3	0.92	1.5	1.15
800	1.3	0.97	1.3	1.10
775	1.3	1.06	1.3	0.98
750	1.2	1.00	1.0	0.81
725	1.0	0.70	0.9	0.74
700	0.8	0.63	0.9	0.67
675	0.8	0.73	0.8	0.77
650	0.7	0.66	0.8	0.60
625	0.8	0.57	0.7	0.55
600	0.8	0.55	0.7	0.48
575	0.9	0.75	0.9	0.77
550	0.9	0.92	0.9	0.96
525	0.9	0.95	0.9	1.01
500	1.0	1.16	1.0	1.16

Table 6. Absolute error analysis of the two interpolation methods for temperature at 0900 GMT. All values are in C°.

Pres (mb)	Time interpolation		New method	
	Mean errors	Standard deviations	Mean errors	Standard deviations
1000	0.7	0.69	0.7	0.63
975	1.7	1.46	1.6	1.53
950	2.1	1.62	1.8	1.14
925	2.2	1.91	1.9	1.32
900	1.8	1.44	1.8	1.42
875	1.4	1.47	1.4	1.46
850	1.1	0.96	1.1	0.99
825	1.3	1.04	1.3	1.09
800	0.9	0.78	1.0	0.75
775	0.9	0.83	0.9	0.75
750	0.9	0.80	0.9	0.80
725	0.8	0.73	0.9	0.70
700	0.9	0.69	0.9	0.71
675	0.7	0.72	0.8	0.81
650	0.7	0.59	0.8	0.62
625	0.6	0.57	0.7	0.62
600	0.7	0.57	0.8	0.57
575	0.7	0.52	0.7	0.47
550	0.8	0.54	0.9	0.56
525	0.7	0.58	0.9	0.71
500	0.8	0.76	0.9	0.84

Table 7. Absolute error analysis of the two interpolation methods for mixing ratio at 0300 GMT. All values are in g/kg.

Pres (mb)	Time interpolation		New method	
	Mean errors	Standard deviations	Mean errors	Standard deviations
1000	1.6	1.07	0.7	0.66
975	1.2	0.98	1.1	0.88
950	1 2	1.13	1.1	0.90
925	1.3	1.19	1.3	1.06
900	1.1	1.10	1.3	1.09
875	1.2	1.21	1.5	1.10
850	1.5	1.40	1.7	1.54
825	1.5	1.35	1.6	1.36
800	1.5	1.34	1.5	1.25
775	1.2	1.22	1.2	1.10
750	1.1	1.26	1.1	0.96
725	1.1	1.27	1.3	1.44
700	1.2	1.36	1.6	1.38
675	0.9	1.02	1.3	0.96
650	0.7	0.79	1.0	0.78
625	0.6	0.61	1.0	0.73
600	0.6	0.47	0.6	0.56
575	0.6	0.58	0.7	0.64
550	0.6	0.57	0.6	0.60
525	0.4	0.37	0.5	0.43
500	0.3	0.27	0.5	0.40

Table 8. Absolute error analysis of the two interpolation methods for mixing ratio at 0600 GMT. All values are in g/kg.

Pres (mb)	Time interpolation		New method	
	Mean errors	Standard deviations	Mean errors	Standard deviations
1000	1.4	0.63	0.6	0.37
975	1.3	1.18	0.8	0.87
950	1.0	0.84	0.9	1.10
925	1.4	1.23	1.3	1.50
900	1.5	1.27	1.4	1.39
875	1.7	1.30	1.7	1.22
850	1.8	1.71	1.9	1.59
825	1.5	1.20	1.5	1.28
800	1.6	1.66	1.6	1.29
775	1.4	1.44	1.3	1.03
750	1.5	1.51	1.5	1.19
725	1.2	1.07	1.6	1.03
700	1.2	1.07	1.7	1.00
675	1.0	0.95	1.4	0.85
650	0.8	0.80	1.1	0.69
625	0.8	0.73	0.8	0.70
600	0.6	0.57	0.8	0.64
575	0.6	0.41	0.7	0.53
550	0.5	0.42	0.7	0.54
525	0.5	0.41	0.5	0.50
500	0.5	0.38	0.5	0.41

Table 9. Absolute error analysis of the two interpolation methods for mixing ratio at 0900 GMT. All values are in g/kg.

Pres (mb)	Time interpolation		New method	
	Mean errors	Standard deviations	Mean errors	Standard deviations
1000	0.9	0.86	0.5	0.47
975	1.2	0.99	0.9	0.51
950	0.9	1.06	0.7	0.47
925	1.4	1.80	1.2	1.94
900	1.3	1.67	1.2	1.87
875	1.4	1.08	1.4	1.20
850	1.6	1.68	1.8	1.53
825	1.7	2.00	1.9	1.82
800	1.3	1.84	1.5	1.69
775	1.2	1.45	1.4	1.25
750	1.0	0.92	1.1	0.82
725	0.9	0.75	1.2	0.73
700	1.1	0.98	1.3	0.88
675	0.7	0.70	1.1	0.74
650	0.8	0.73	1.1	0.64
625	0.8	0.82	1.0	0.79
600	0.7	0.67	0.9	0.78
575	0.6	0.50	0.8	0.61
550	0.5	0.49	0.6	0.51
525	0.4	0.44	0.5	0.45
500	0.4	0.34	0.5	0.36

levels. Also when comparing the errors associated with the new method applied to separated storm and non-storm cases, there was no distinct advantage found to separation of the cases over performing the interpolation without regard to storm or non-storm sounding. Consequently the combined interpolation technique without separating the soundings was used in the remainder of this study.

Stability Indices

The four MCC cases for the study are listed in Table 10. In these four cases, on average, nine rawinsonde stations were included in the study of each case. Case 1 contained seven stations which was the smallest number while Case 4 had 13 stations.

Table 10. Mesoscale Convective Storm Systems (MCSs) included in study. Initiate and terminate times are after Maddox et al. (1982), Rodgers et al. (1983, 1985).

Case number	Date	Initiate	Maximum extent *	Terminate
1	10/11 Apr 81	2315/10	0300/11	0531/11
2	9 May 81	0115/09	0500/09	1015/09
3	17 May 82	0030/17	0400/17	0730/17
4	10/11 Jun 82	2245/11	0700/11	1530/11

*The times listed are the maximum extent of the area, as depicted on IR satellite imagery, with temperatures $\leq$ -62 C.

After the interpolated soundings were obtained, a variety of stability indices were examined. These were the K, modified K, Total-Totals, modified Total-Totals, CAPE, and Showalter indices along with the maximum rate of decrease of equivalent potential temperature over a 25 mb layer from the surface to 700 mb (PII- Potential Instability Index). The difference between the modified and the regular versions of the K and Total-Totals indices is that in the modified versions, the moisture was averaged between the surface and 850 mb for determination of a dewpoint temperature to be used at 850 mb. In the standard versions, the observed 850 mb dewpoint is used. The justification for this approach is that in many of the soundings, the moisture was confined to the layer below 850 mb. So, the value of the standard index could be misleading in terms of its accounting for lower tropospheric moisture.

After calculating, plotting and examining the fields of these indices, the standard versions of the K and Total-Totals indices along with the CAPE were discarded. The reason for dropping the K and Total-Totals indices was that the fields of these indices were similar in nature to the fields plotted from the modified versions Also, it was felt that that the modified versions were more representative of the actual stability of the atmosphere. The CAPE index, which is a measure of the positive area of the sounding when plotted on a Skew-T, Log-P diagram, was small or even zero throughout the plotted fields. This result is not surprising since the stabilizing effect of nocturnal, radiative cooling was present in the boundary layer.

The Environmental Airflow

To show the airflow in the atmosphere around the MCC, the winds at approximately 1 km above the surface at 00 and 12 GMT were obtained from the rawinsondes. This level was chosen because it is thought to be near the top of the boundary layer and therefore indicates the flow, free of friction, whose stability may be affecting the storm. To get the winds at 03, 60, and 09 GMT, linear time interpolation between the 00 and 12 GMT wind values was used. The movement of each storm was determined from enhanced infrared, satellite images. This motion vector was then subtracted from the 1 km winds to get the storm-relative wind vectors.

Results for Case 1

The analyses of the four cases listed in Table 10 are incomplete at this time. Some of the results for Case 1 are available and are discussed below.

Figures 1a,b,and c deal with the field of modified K index at 00, 03, and 06 GMT, respectively. It can be seen in Table 10 that these times correspond to 45 min after MCC initiation, the time of maximum extent, and 29 min after MCC termination, respectively. Termination refers only to the time that the storm ceased to qualify as an MCC, and not to its actual demise.

In Fig. 1a, the storm position is indicated by the heavy lines indicating the IR equivalent black-body temperature field at the top of the storm. The storm-relative velocity vectors in knots are shown for selected stations and the thin lines represent the modified K values. Figures 1b and 1c show the same quantities. Several features can be observed by a

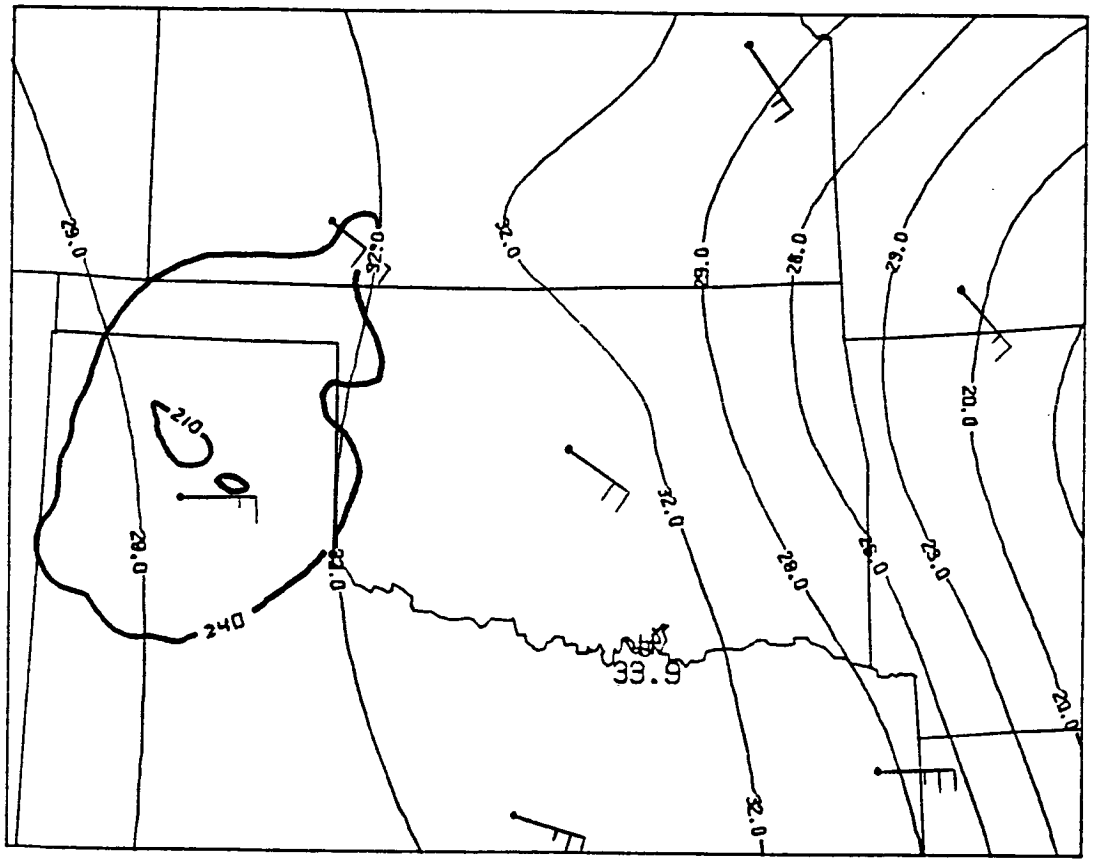

Fig. 1a. Modified K index field for 0000 GMT 11 April 1981.

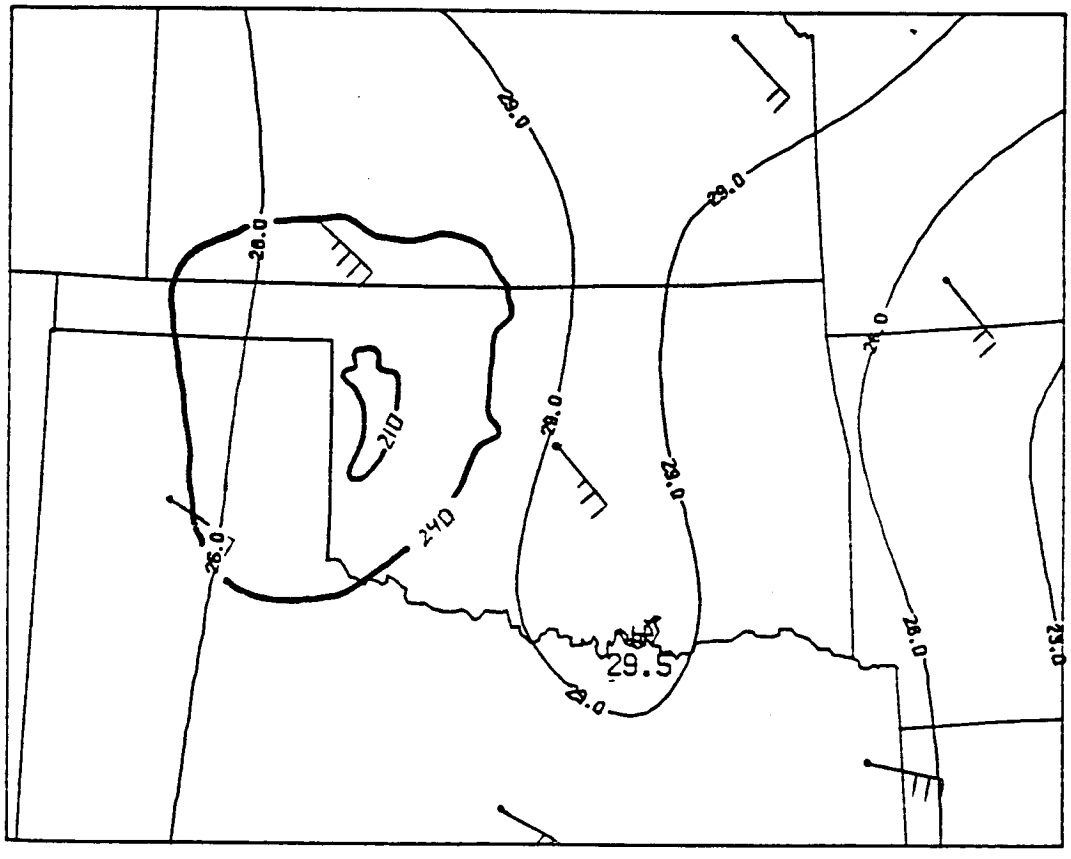

Fig. 1b. Same as Fig. 1a except for 0300 GMT.

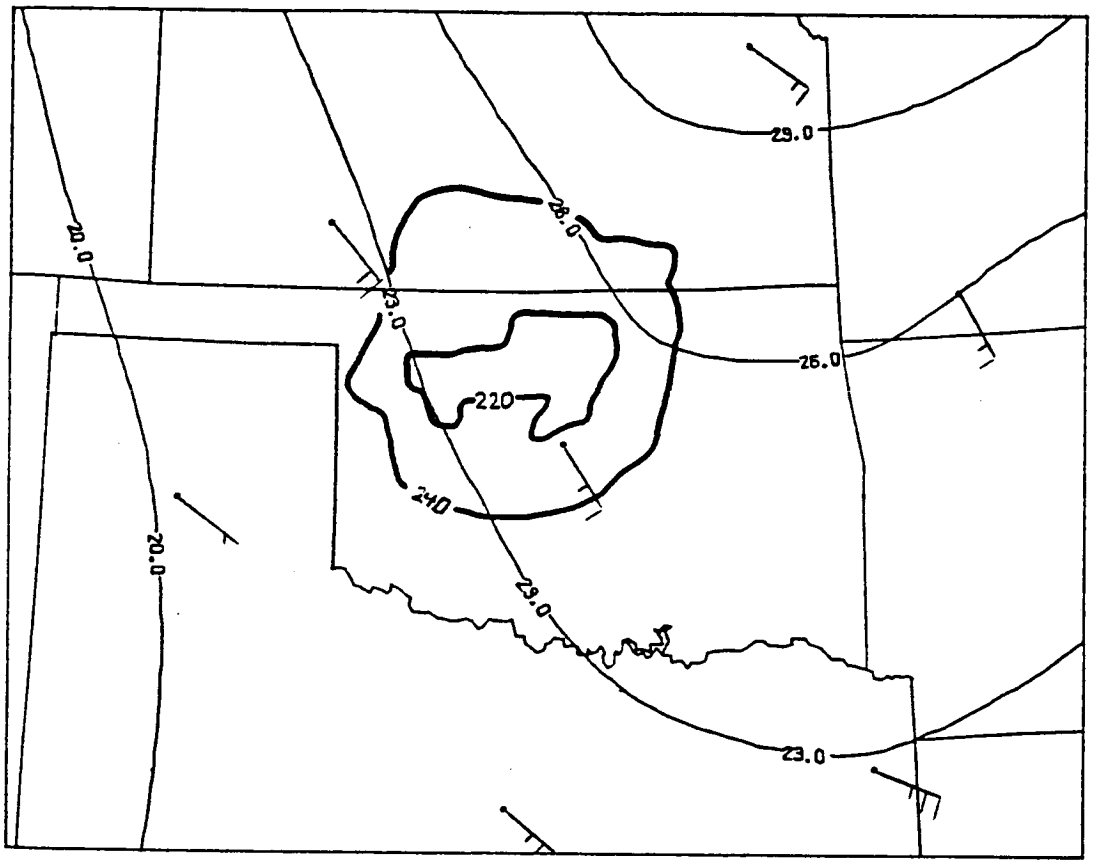

Fig. 1c. Same as Fig. 1a except for 0600 GMT.

comparison of these three figures. First, it is noted that throughout this 6-h period, there is an axis or ridge of larger modified K values to the east of the storm. However, as time goes on, there is a generalized decrease of modified K values across the entire area. This reflects the stabilizing influence of the nocturnal cooling. The relative flow at 00 and 03 GMT indicated an apparent advection of less stable air into the storm area which would seem to explain why the storm reached its maximum extent at 03 GMT. However, a visual examination of the modified K values contained within the 240°K isotherm at each time reveals that the approximate average value went from about 30 at 00 GMT to 27 at 03 GMT and then to about 24.5 at 06 GMT. Thus, it would appear that the radiation effect dominated over the advection effect so that even as the storm was approaching maximum intensity, it was self-destructing in the sense that it was drawing in more-stable air.

Figures 2a b,and c show the situation for the stability field based on the modified Total-Totals index. These figures indicate an altogether different situation than seen in Figures 1a-c. In these figures the most unstable region is to the northwestern side of the storm at 00 and 03 GMT and to the northeast and southwest of the storm at 06 GMT. The relative flow throughout the time period indicates an apparent advection of more stable air into the storm area. A general diminishing of stability across the area occurs only in the period from 03 to 06 GMT. The most unstable approximate storm average value corresponds to the time of maximum extent at 03 GMT. So in this case, the modified Total-Totals field did not

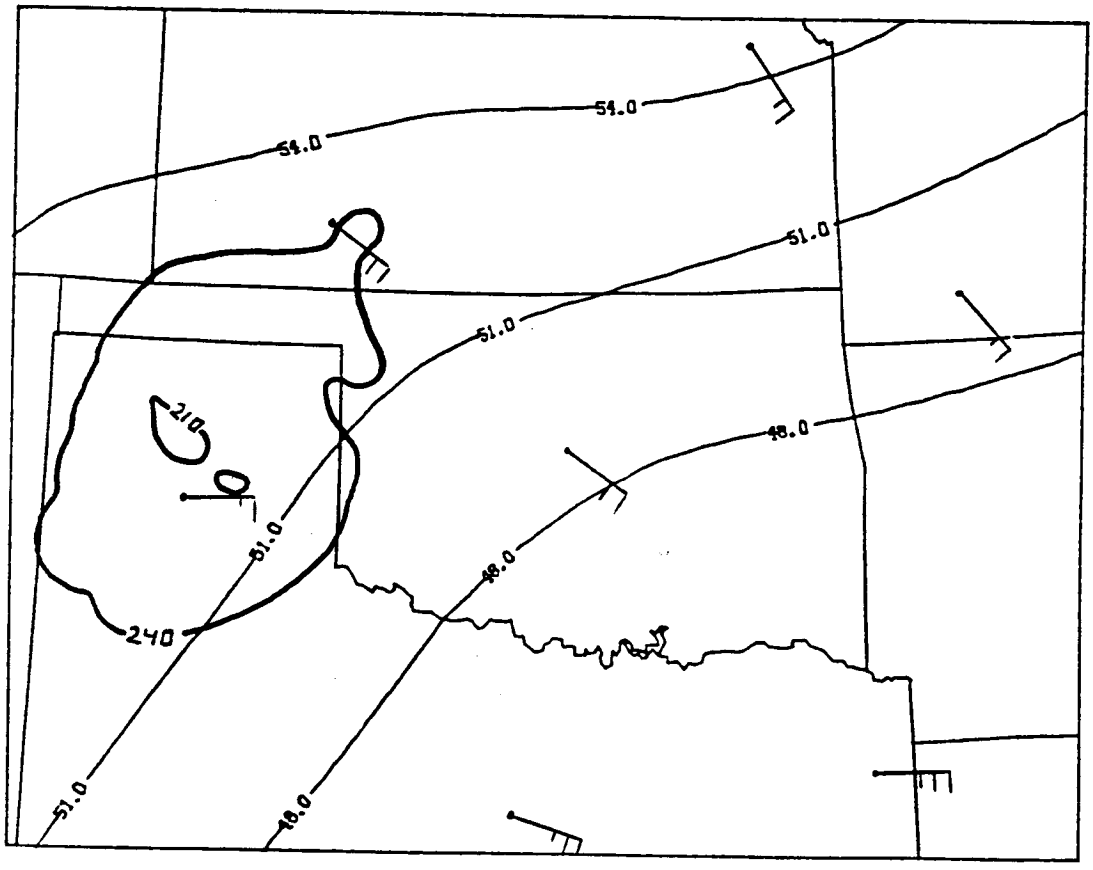

Fig. 2a. Modified Totals-Totals index field for 0000 GMT 11 April 1981.

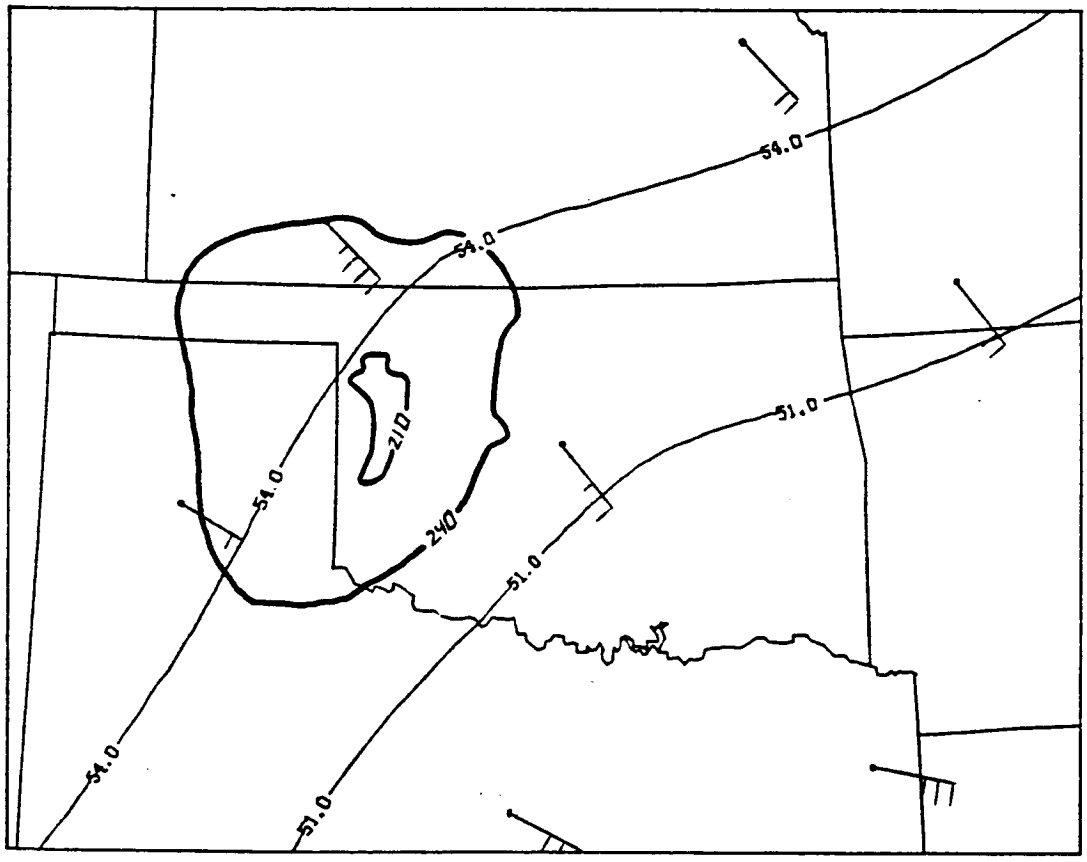

Fig. 2b. Same as Fig. 2a except for 0300 GMT.

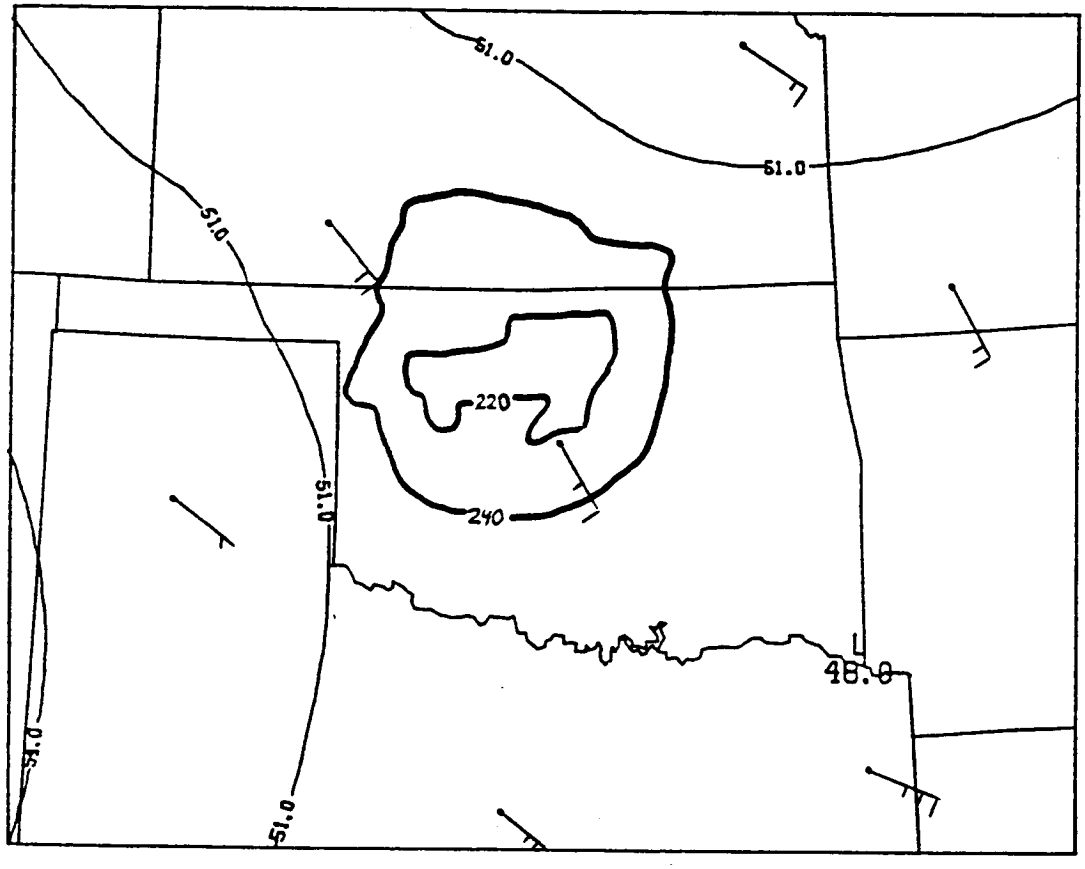

Fig. 2c. Same as Fig. 2a except for 0600 GMT.

immediately indicate the stabilizing effect of nocturnal cooling.

The Showalter index stability fields at 00 through 06 GMT are shown in Figures 3a,b,and c, respectively. These figures show a similar situation to that shown in Figures 2a-c. The most unstable regions from 00 to 06 GMT are located to the north and south of the storm. The relative flow at 00 GMT indicates that the apparent advection at this time is small but is probably moving slightly less-stable air towards the storm area. At 03 and 06 GMT, the apparent advection again is small but indicated movement of somewhat more stable air into the storm area. This initiation in the apparent advection of more stable air into the storm corresponds to the time of maximum extent. The approximate average of the Showalter index within the 240°K isotherm went from about -0.5 at 00 GMT to about -2.0 at 03 GMT and then to -1.0 at 06 GMT. Thus, the most unstable value again corresponded to the time of maximum extent. Again, the effect of the nocturnal cooling in the lower troposphere was not reflected in the Showalter field until 06 GMT.

The PII (Potential Instability Index) stability field is depicted in Figures 4a,b,and c for 00, 03, and 06 GMT, respectively. The most unstable air, according to this index, is located to the north of the storm with an axis of less-stable air to the east of the storm. This axis shifts somewhat westward with time while the storm moves northwestward until it becomes located on the axis at 06 GMT. Also during this period, the entire field of PII undergoes a modification in values indicating greater stability with

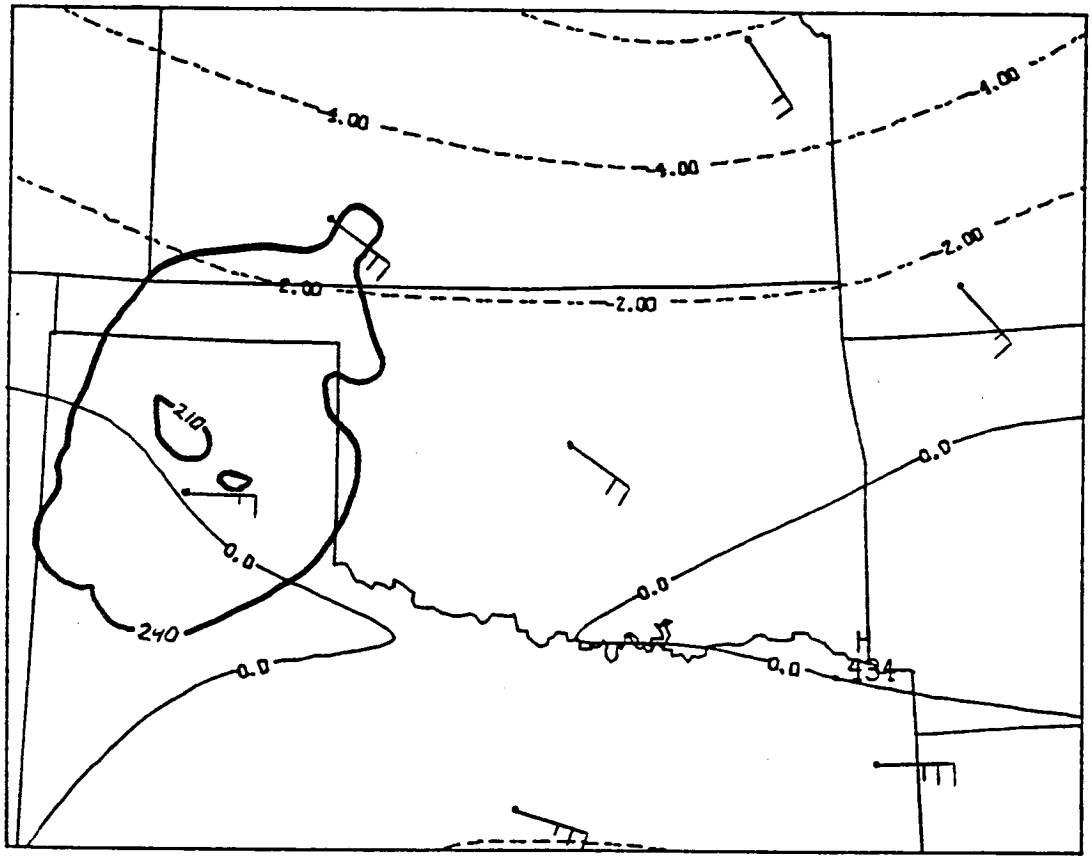

Fig. 3a. Showalter index field for 0000 GMT 11 April 1981.

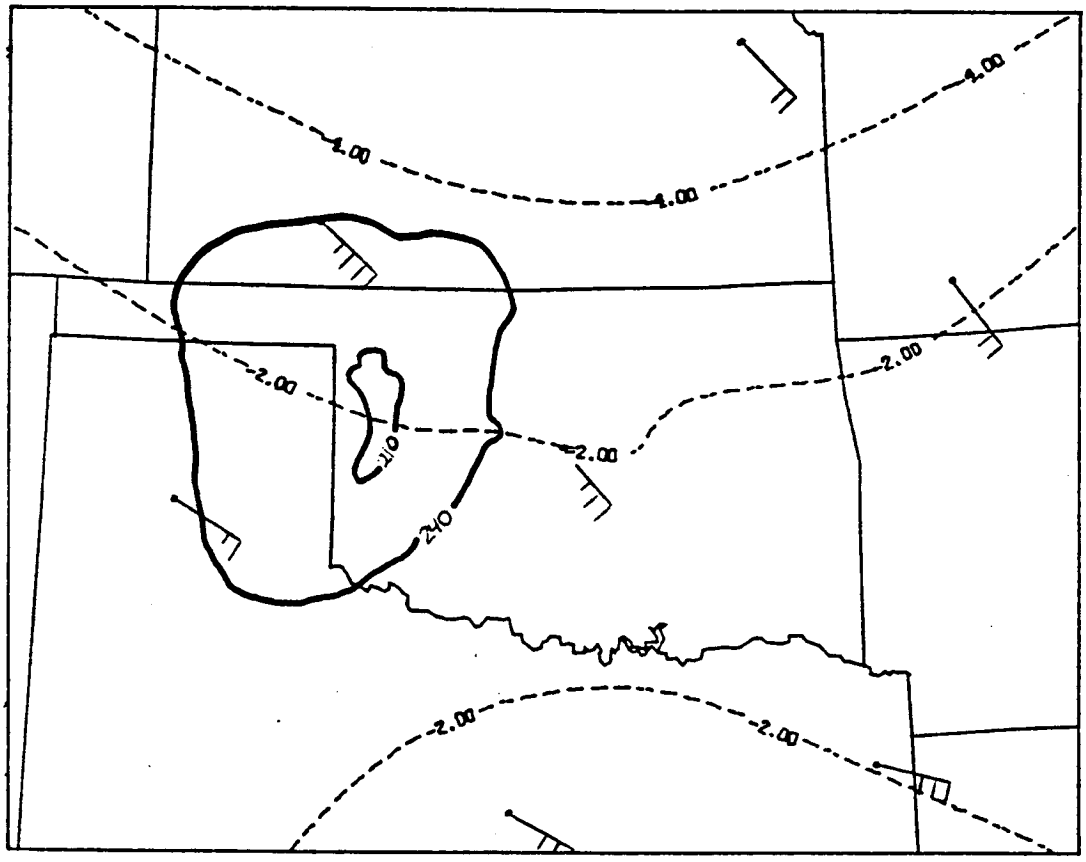

Fig. 3b. Same as Fig. 3a except for 0300 GMT.

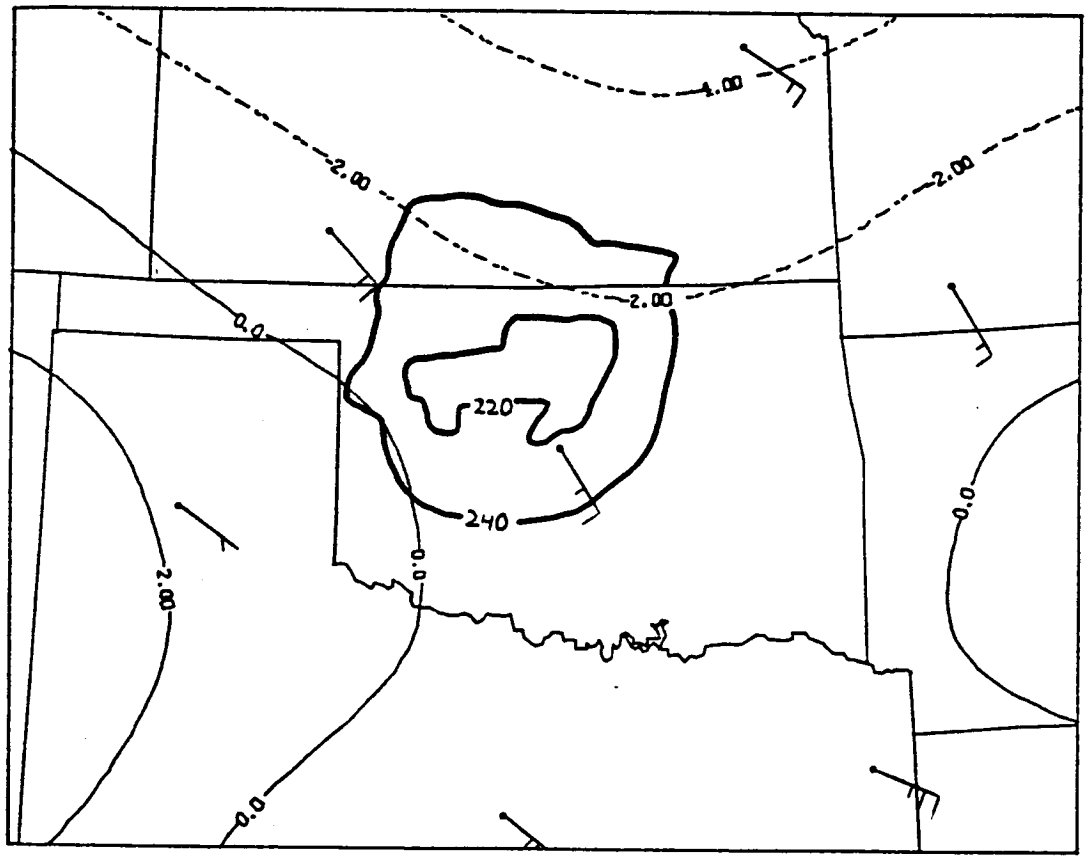

Fig. 3c. Same as Fig. 3a except for 0600 GMT.

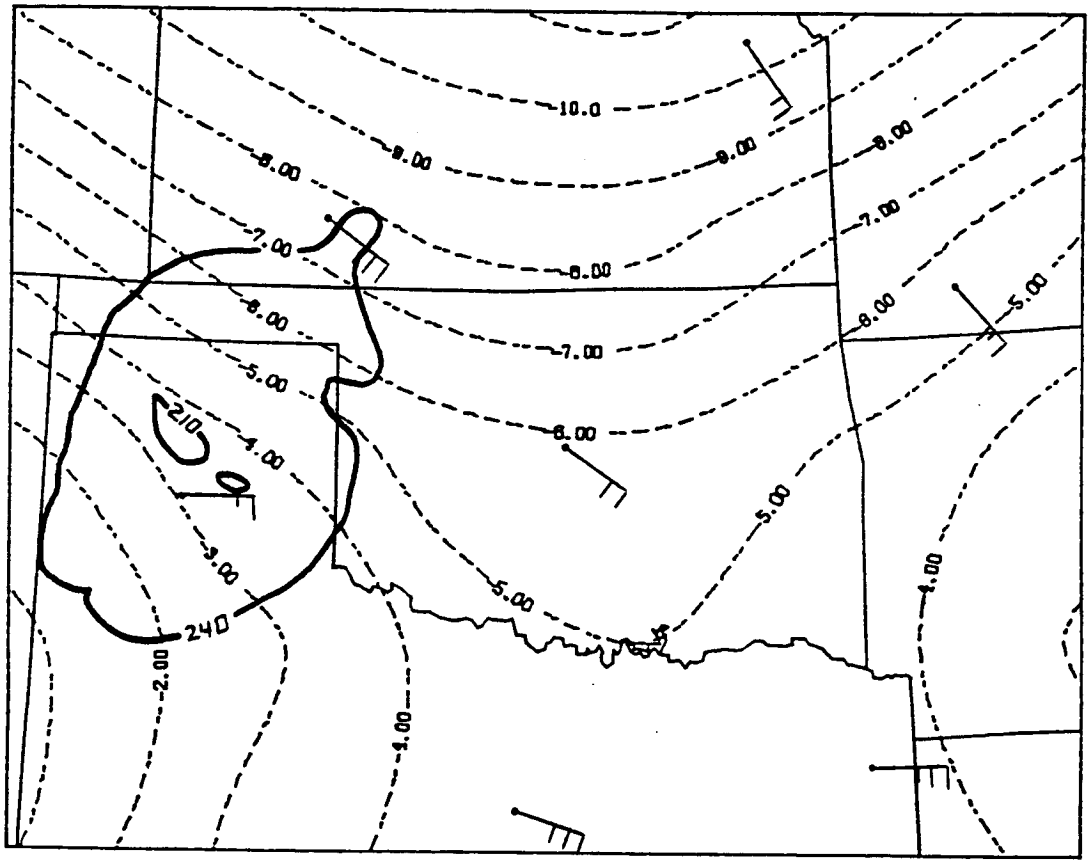

Fig. 4a. Potential Instability Index field for 0000 GMT 11 April 1981.

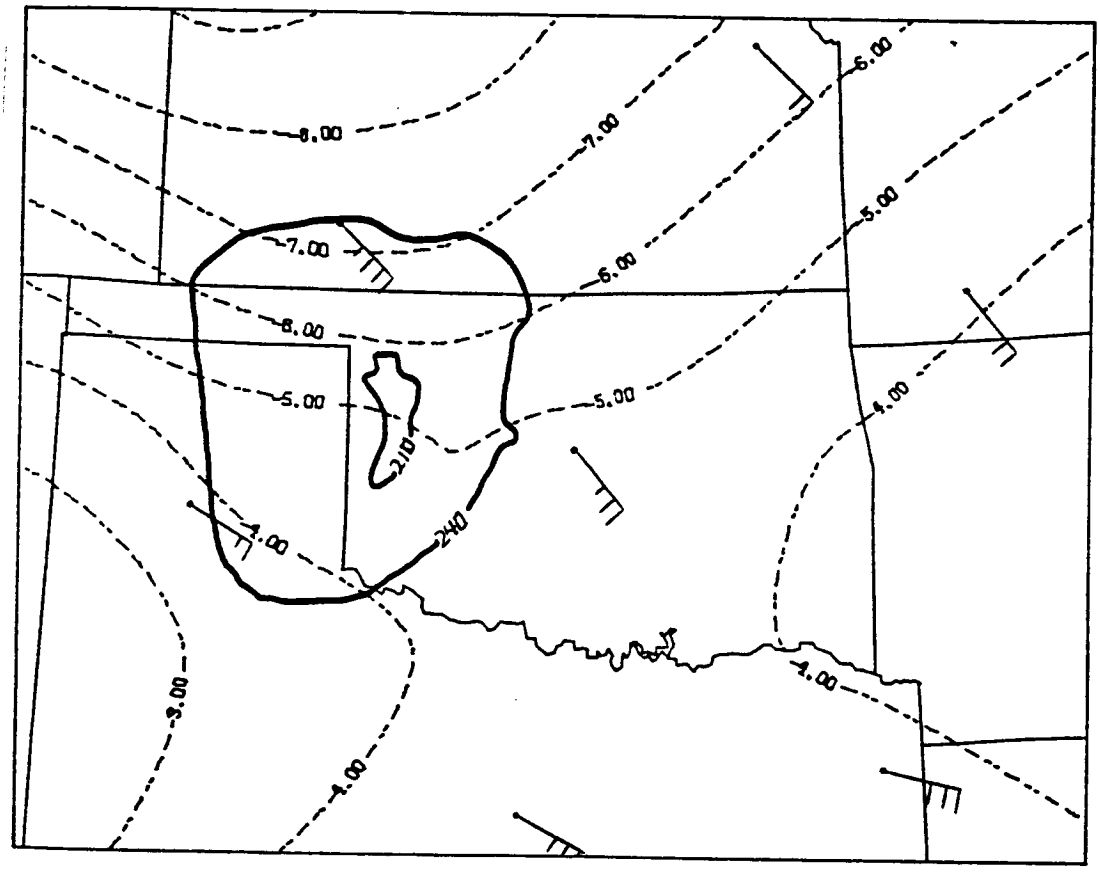

Fig. 4b. Same as Fig. 4a except for 0300 GMT

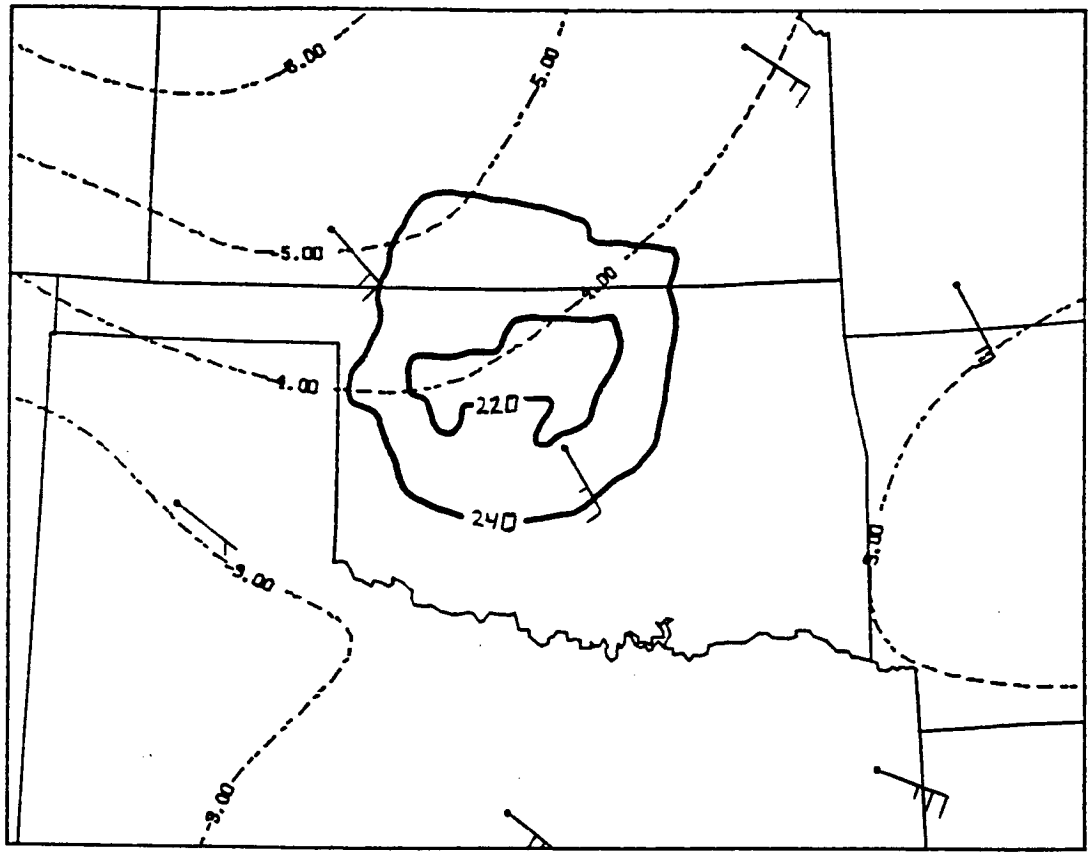

Fig. 4c. Same as Fig. 4a except for 0600 GMT.

time.

At 00 GMT, the average PII value within the 240 K isotherm was approximately -4.5. By 03 GMT, this average has decreased to about -5.5 meaning the area was slightly less-stable. Finally, at 06 GMT, the average was about -4.0. These changes in internal stability correspond nicely with the intensity changes in the storm. The relative flow at 00 GMT suggests a weak flux of less-stable air into the storm. But at 03 and 06 GMT, the flow suggests an apparent flux of stable air into the storm area. Again, this corresponds well to the observed intensity variations of the MCC.

IV. TENTATIVE CONCLUSIONS

One would expect that regardless of the structure of the stability field provided by any of the given indices that certain changes and relationships should be observed to occur during the lifetime of the MCC. These are:

1. The stabilizing influences of the nocturnal radiative cooling should be reflected in the overall stability field becoming more stable with time.
2. The stability within the storm boundary should be reflected in the intensity changes in the storm. Thus, the time of maximum extent of the storm should occur near the time of maximum instability in the storm. Increasing stability of the air in the storm should lead to diminished storm intensity.
3. The storm-relative flow should indicate a flux of less-stable air into the storm as it approaches its most intense stage and a flux of more-stable air into the storm as its termination time is approached.

In fact, the four stability indices examined here differed from one another in some of these aspects while agreeing in others. Only the Potential Instability Index (PII) met expectations in every category listed above. The reason for this is probably a consequence of the quantities which go into the calculation of each of these indices and the extent to which they become modified by the lower tropospheric stabilization provided by the interpolation scheme. The solution to this problem requires additional analysis of Case 1 and the comparison with results from the other

cases under study.

V. REFERENCES

Byers, H. R. 1944: General Meteorology., McGraw-Hill, Inc., New York, NY, 461 pp.

Dupuis, L. R. and J. R. Scoggins, 1979 Differences between measured linearly interpolated synoptic variables over a 12-h period during AVE IV. NASA CR-3150, NASA Marshall Space Flight Center, Huntsville, AL, 126 pp.

Fritsch, J. M., R. A. Maddox and A. G. Barnstron, 1981: The character of mesoscale convective complex precipitation and its contribution to warm season rainfall in the U. S. Preprints, 4th Conf. on Hydrometeorology, Reno, NV, Amer. Meteor. Soc., 94-99.

House, D. C., 1960: Remarks on the optimum spacing of upper air observations. Mon. Wea. Rev., 88, 97-100.

Kreitzburg, C. W. and H. A. Brown, 1970: Mesoscale weather systems within an occlusion. J. Appl. Meteorol., 9, 417-432.

Maddox, R. A. 1980: Mesoscale convective complexes. Bull. Amer. Meteor. Soc., 61, 1374-1387.

_____ 1981: The structure and lifecycle of midlatitude mesoscale convective complexes. Atmos. Sci. Pap. No. 336, Colorado State University 311 pp.

_____, D M. Rodgers and K. W. Howard, 1982: Mesoscale convective complexes over the United States during 1981. Mon. Wea. Rev. 110, 1501-1514.

Overall, J. W. and J. R. Scoggins, 1975: Relationships between motion on isentropic surfaces from 3-h rawinsonde data and radar echoes. NASA CR-2558, NASA Marshall Space Flight Center, Huntsville, AL, 111 pp.

Read, W. L and J. R. Scoggins, 1977: Vorticity imbalance and stability in relation to convection. NASA CR-2819, NASA Marshall Space Flight Center, Huntsville, AL, 111 pp.

Rodgers, D. M., K. W. Howard and E. C. Johnston, 1983. Mesoscale convective complexes over the United States during 1982. Mon. Wea. Rev., 111, 2363-2369.

_____, M. J. Magnano and J. H. Arns, 1985: Mesoscale convective complexes over the United States during 1983. Mon. Wea. Rev., 113, 888-901.

Welshinger, M. J., 1985: Factors leading to the formation of arc cloud complexes. Masters Thesis, Texas A&M Univ., College Station, TX, 110 pp.

Wilson, G. S. and J. R. Scoggins, 1976: Atmospheric structure and variability in areas of convective storms determined from 3-h rawinsonde data NASA CR-2678, NASA Marshall Space Flight Center, Huntsville, AL, 118 pp.